Operational Bottleneck Identification Based Energy Storage Investment Requirement Analysis for Renewable Energy Integration

Siyuan Wang, Guangchao Geng, *Senior Member, IEEE,* Junchao Ma, Quanyuan Jiang, *Senior Member, IEEE,* Hongyang Huang, and Boliang Lou

***Abstract*—Operational bottlenecks are commonly observed in power systems and lead to severe system security issues, which may be caused by the fluctuating and uncertain nature of renewable energy. This paper presents an approach to define, identify and eliminate such bottlenecks in the scope of system balance for renewable energy integrated bulk power systems, so as to quantify the requirement of energy storage. A mixed-integer linear programming (MILP) formulation for system operational bottleneck identification is proposed given renewable generation profile, in order to obtain operational restriction indices to assess the adequacy of power adjustment margin and power ramp rate. Cosine similarity based density-based spatial clustering of applications with noise (DBSCAN) method is used to cluster a large number of scenarios by operational restriction indices, then scenarios with bottlenecks are attributed to corresponding clusters. Finally, various bottleneck elimination options, including energy storage with different technologies, are compared for each cluster. Case studies of an eight-bus test system and a practical Chinese power system are presented to verify the proposed approach, the numerical results indicate energy storage is the most effective option to eliminate bottlenecks identified in power downward adjustment margin and ramp rate dominated clusters aforementioned.**

***Index Terms*—bottleneck identification, clustering, renewable energy, energy storage.**

NOMENCLATURE

Indices and Sets

i	Index of equipment in power systems
t	Index of time slots
s	Index of scenarios
l	Index of points in a start-up (shut-down) trajectory
Ω_{w}	Set of wind farms or solar stations
Ω_{d}	Set of loads
$\Omega_{\mathrm{g}}, \Omega_{\mathrm{chp}}$	Set of generators or CHP generators

Parameters

N_t	Number of time slots
Δt	Interval of a dispatch time slot
$W_{i,t}$	Power of renewable energy source i at time t
$D_{i,t}$	Power of load i at time t
RU_i, RD_i	Ramp up or ramp down ability of generator i
$\overline{P}_i, \underline{P}_i$	Maximum or minimum output of generator i
RU_i^{SU}, RD_i^{SD}	Upward or downward ramp rate at start-up or shut-down phase of generator i
$T_i^{\mathrm{SU(DSD)}}$	Start-up (shut-down) time of generator i
UT_i, DT_i	Minimum online or offline time of generator i
$V_{i,0}, S_{i,0}$	Initial online or offline time of generator i
$u_{i,0}$	Initial on/off status of generator i
$c_i^{\mathrm{v1}}, c_i^{\mathrm{v2}}$	Slope for power upper or lower bound of CHP generator i
c_i^{m}	Slope for back pressure curve of CHP generator i
ϕ_i	Electric power axis intercept for back pressure curve of CHP generator i
$h_{i,t}$	Heat power output of CHP generator i at time t

Decision Variables

$p_{i,t}$	Power output of generator i at time t
$v_{i,t}, w_{i,t}$	Start-up or shut-down status of generator i at time t
$u_{i,t}$	On/off status of generator i at time t
$\hat{p}_{i,t}$	Power output above the minimum output of generator i at time t
$\lambda_i^{(\cdot)}$	Slack variables of generator i
$\lambda^{(\cdot)}$	System operational restriction indices

Manuscript received October 20, 2019; revised February 21, 2020; accepted March 19, 2020. This work was supported in part by State Grid Zhejiang Electric Power Co. Ltd. Science and Technology Research Grant (5211DS18003A) and National Natural Science Foundation of China (51677164). Paper no. TSTE-01135-2019. *(Corresponding author: Guangchao Geng.)*

Siyuan Wang was with College of Electrical Engineering, Zhejiang University, Hangzhou 310027, China. He is now with Department of Electrical and Computer Engineering, Missouri University of Science and Technology, Rolla, MO 65409, USA (e-mail: sywang@zju.edu.cn; siyuanwang@mst.edu).

Guangchao Geng and Quanyuan Jiang are with College of Electrical Engineering, Zhejiang University, Hangzhou 310027, China (e-mail: ggc@zju.edu.cn; jqy@zju.edu.cn).

Junchao Ma, Hongyang Huang and Boliang Lou are with State Grid Zhejiang Electric Power Research Institute, Hangzhou 310014, China.

I. INTRODUCTION

WITH increasing penetration of wind and solar generation in power systems worldwide, challenges have been encountered on system balance because of the fluctuating and uncertain nature of renewable energy. What is worse, extreme cases like solar eclipse [1], and wind power ramp events in both onshore [2], [3] and offshore [4] wind farms, are more frequently reported to threat system security, which leads to significant bottlenecks in the system operation. Energy storage technology is believed to be a promising option to address such issues, and has garnered increasing attention in recent years. Therefore, it is an urgent need to establish a systematic

This article has been accepted for publication in IEEE Transactions on Sustainable Energy. DOI: 10.1109/TSTE.2020.2984651.

approach to define, identify and eliminate operational bottlenecks, this is especially important to understand the role of energy storage and quantify its benefit in alleviating such bottlenecks.

In recent literature, the use of energy storage technology has been widely investigated in renewable energy integrated power systems. Storage operation and planning approaches for power system peak load shifting were proposed in [5]–[7] considering renewable power uncertainties. Battery energy storage system control strategies were proposed to mitigate wind farm fluctuations and address wind power ramp events in [8], [9]. Results of [10], [11] illustrated system operational cost and generator commitment counts can be reduced with the presence of energy storage. The above literature demonstrates that energy storage systems are able to shift peak and valley load, control wind power ramp events and alleviate frequent start-up and shut-down behavior of generators. However, due to the relatively high price of some types of utility-scale energy storage stations in bulk power systems, seldom studies address the cost-effectiveness issue of energy storage compared with existing technological options, such as conventional generators.

In this paper, a systematic framework is proposed to assess the existence, type, and severity of system operational bottlenecks for different scenarios, and then investigate energy storage investment requirements for different bottleneck types. The procedure consists of system operational bottleneck identification, operational restriction indices based scenario clustering and cost-effectiveness comparative analysis of energy storage investment.

To identify system bottlenecks, various studies have been conducted in related research fields. A bottleneck identification for corridor management planning in transportation systems was proposed in [12]. A bottleneck identification method was developed for urban traffic networks under different traffic demands in [13]. For the risk management of supply chain networks, a bottleneck identification method was investigated in [14]. An algebraic approach to identify bottlenecks in continuous process systems is presented in [15], which is designed to produce a particular product portfolio. However, such methods have seldom been extended to power system operations with renewable energy integration. The aim of developing an operational bottleneck identification method in this work is to characterize system weakness by operational restriction indices.

Scenario clustering methods have been widely used to deal with the stochastic nature of renewable generation in the literature. In the stochastic wind farm investment problem of [16], the representation of the correlative load and wind power was achieved by applying the k-means clustering technique on load and wind curves. The DBSCAN method was used to eliminate stacked outliers in [17] for a wind farm power curve refining problem. In the area of dynamic voltage control, the spectral clustering algorithm was used in [18] to classify dynamic contingencies into different clusters according to their behavioral patterns. In [19], a DBSCAN based method is applied to determine stepwise electricity consumption levels for residential areas. In light of the aforementioned works, we extend the idea to our scenario clustering problem based on operational restriction indices, in order to conduct cost-effectiveness comparisons for energy storage under different bottleneck clusters. We use the DBSCAN method because it is not required to pre-specify the number of clusters. In addition, an appropriate distance metric is defined for scenario clustering.

The main contributions of this work include:

1) For renewable energy integrated bulk power systems, an approach to define, identify and eliminate system operational bottlenecks in the scope of system balance is proposed. Conclusion on the cost-effectiveness of energy storage investment on bottleneck elimination is made.
2) An MILP formulation is established to identify system operational bottlenecks under given renewable generation and load profile. It also calculates operational restriction indices to quantify the system bottlenecks.
3) We define a cosine similarity based metric to measure the similarity of bottlenecks for any two scenarios. A DBSCAN based scenario clustering method is applied to our application to avoid pre-specify the number of clusters.

II. Operational Bottleneck Identification

An MILP formulation for system operational bottleneck identification is established to find operational bottlenecks in the scope of system balance. The model is adapted from operational models that consider system balance and main operational features of generators, i.e., capacity limits, ramp limits, minimum online and offline time limits. However, some challenges still remain to construct an effective and computationally efficient operational bottleneck identification formulation. The problem formulation, feasibility analysis, and constraint linearization are presented in this section.

A. Problem Formulation

1) System Constraints: Equation (1) ensures system power balance at each time period.

$$\sum_{i\in\Omega_{\mathrm{g}}\bigcup\Omega_{\mathrm{chp}}} p_{i,t}+\sum_{i\in\Omega_{\mathrm{w}}} W_{i,t}=\sum_{i\in\Omega_{\mathrm{d}}} D_{i,t}\quad \forall t \tag{1}$$

2) Generator Constraints: Generator constraints are relaxed based on the formulation that takes start-up and shut-down ramp trajectories into account [20], [21]. Slack variables are added to the main technical parameters of generators, which indicates system bottleneck will be eliminated if the corresponding parameter is improved by its slacked value. The technical parameters to be slacked are maximum power output $\overline{P}_i$, minimum technical power output $\underline{P}_i$, upward ramp rate limit RU_i, and minimum ramp rate limit RD_i. Slack variable values for them correspond to system bottlenecks on generation capacity, downward power adjustment margin (including flexible start-up and shut-down), upward ramp rate limit and downward ramp rate limit, respectively. Note the parameters of minimum online time UT_i and offline time DT_i are not relaxed in the formulation. The reason is that flexible start-up and shut-down bottlenecks can be identified

by relaxing the minimum technical power output $\underline{P}_i$. If the minimum technical power output of a generator decreases, some shut-down and start-up behaviors would be avoided. In an extreme case, suppose $\lambda_i^{\text{PMIN}} = \underline{P}_i$, i.e., the minimum technical power is zero, the output could be zero even when the commitment status is on ($u_{i,t} = 1$). In other words, a generator can behave like there is no start-up and shut-down restrictions if its minimum technical power output is zero.

$$u_{i,t+1} - u_{i,t} = v_{i,t+1} - w_{i,t+1} \quad \forall i \in \Omega_{\text{g}}, t \tag{2}$$

$$v_{i,t} + w_{i,t} \leq 1 \quad \forall i \in \Omega_{\text{g}}, t \tag{3}$$

$$0 \leq \hat{p}_{i,t} \leq \left[\left(\overline{P}_i + \lambda_i^{\text{PMAX}}\right) - \left(\underline{P}_i - \lambda_i^{\text{PMIN}}\right)\right] u_{i,t} \quad \forall i \in \Omega_{\text{g}}, t \tag{4}$$

$$-\left(RD_i + \lambda_i^{\text{RD}}\right) \cdot \Delta t \leq \hat{p}_{i,t+1} - \hat{p}_{i,t} \leq \left(RU_i + \lambda_i^{\text{RU}}\right) \cdot \Delta t \quad \forall i \in \Omega_{\text{g}}, t \in [1, N_t - 1] \tag{5}$$

$$\begin{aligned} p_{i,t} = {} & \hat{p}_{i,t} + \left(\underline{P}_i - \lambda_i^{\text{PMIN}}\right) u_{i,t} \\ & + \sum_{l=1}^{T_i^{\text{DSU}}} \left[RU_i^{\text{SU}} \cdot \Delta t \cdot l - \lambda_i^{\text{PMIN}}\right]^+ \cdot v_{i,t+T_i^{\text{DSU}}-l+1} \\ & + \sum_{l=1}^{T_i^{\text{DSD}}} \left[\left(\underline{P}_i - RD_i^{\text{SD}} \cdot \Delta t \cdot (l-1)\right) - \lambda_i^{\text{PMIN}}\right]^+ \cdot w_{i,t-l+1} \\ & \forall i \in \Omega_{\text{g}}, t \end{aligned} \tag{6}$$

$$\begin{cases} \sum_{t=1}^{G_i} (1 - u_{i,t}) \leq 0 \quad \forall i \in \Omega_{\text{g}} \\ \sum_{n=t}^{t+UT_i-1} u_{i,n} \geq UT_i \cdot v_{i,t} \\ \qquad \forall i \in \Omega_{\text{g}}, t \in [G_i + 1, N_t - UT_i + 1] \\ \sum_{n=t}^{N_t} (u_{i,n} - v_{i,t}) \geq 0 \quad \forall i \in \Omega_{\text{g}}, t \in [N_t - UT_i + 2, N_t] \\ G_i = \min\left\{N_t,\ \max\left\{0,\ \left(UT_i - V_{i,0}\right) u_{i,0}\right\}\right\} \end{cases} \tag{7}$$

$$\begin{cases} \sum_{t=1}^{L_i} u_{i,t} \leq 0 \quad \forall i \in \Omega_{\text{g}} \\ \sum_{n=t}^{t+DT_i-1} (1 - u_{i,n}) \geq DT_i \cdot w_{i,t} \\ \qquad \forall i \in \Omega_{\text{g}}, t \in [L_i + 1, N_t - DT_i + 1] \\ \sum_{n=t}^{N_t} (1 - u_{i,n} - w_{i,t}) \geq 0 \\ \qquad \forall i \in \Omega_{\text{g}}, t \in [N_t - DT_i + 2, N_t] \\ L_i = \min\left\{N_t,\ \max\left\{0,\ \left(DT_i - S_{i,0}\right)\left(1 - u_{i,0}\right)\right\}\right\} \end{cases} \tag{8}$$

$$0 \leq \lambda_i^{\text{PMAX}},\ 0 \leq \lambda_i^{\text{PMIN}} \leq \underline{P}_i,\ 0 \leq \lambda_i^{\text{RD}},\ 0 \leq \lambda_i^{\text{RU}} \quad \forall i \in \Omega_{\text{g}} \tag{9}$$

Equation (2) represents the relation between up/down statuses and online/offline statuses. Equation (3) establishes the disjunctive logic relation between start-up and shut-down statuses. Equation (4) limits the operational upper and lower bounds for each online unit. In (4), the parameters of maximum power output $\overline{P}_i$ and minimum technical power output $\underline{P}_i$ are slacked, which introduces the nonlinear product terms of the slack variables $\lambda_i^{\text{PMAX}}(\lambda_i^{\text{PMIN}})$ and the online status binary variables $u_{i,t}$. Equation (5) provides the ramp limit with upward ramp limit RU_i and minimum ramp limit RD_i slacked. The network injection power is presented in (6), wherein the maximum power output parameter is slacked. Equation (6) not only introduces a piecewise function to avoid negative value in start-up and shut-down trajectories, but also contains product terms of piecewise functions and binary variables that represent up/down statuses. Equation (7) and (8) correspond to minimum online and offline time limits, respectively. Equation (9) provides bounds for slack variables.

As a special category of thermal generators, the combined heat and power (CHP) generator operates to provide heat supplies in the heating season, i.e., late autumn, winter, and early spring. CHP units are assumed to be constantly online during the heating season, therefore (2)-(9) can be modified with fixed commitment states and heat-power-related electric power bounds. Equations (10)-(12) represent limits for power outputs [22], ramp rates and slack variables, respectively.

$$\begin{aligned} \max\left\{\underline{P}_i - c_i^{\text{v2}} h_{i,t} - \lambda_i^{\text{PMIN}},\ c_i^{\text{m}} h_{i,t} + \phi_i - \lambda_i^{\text{PMIN}},\ 0\right\} & \leq p_{i,t} \\ \leq \left(\overline{P}_i - c_i^{\text{v1}} h_{i,t} + \lambda_i^{\text{PMAX}}\right) & \quad \forall i \in \Omega_{\text{chp}}, t \end{aligned} \tag{10}$$

$$-\left(RD_i + \lambda_i^{\text{RD}}\right) \cdot \Delta t \leq p_{i,t+1} - p_{i,t} \leq \left(RU_i + \lambda_i^{\text{RU}}\right) \cdot \Delta t \quad \forall i \in \Omega_{\text{chp}}, t \in [1, N_t - 1] \tag{11}$$

$$0 \leq \lambda_i^{\text{PMAX}},\ 0 \leq \lambda_i^{\text{PMIN}},\ 0 \leq \lambda_i^{\text{RD}},\ 0 \leq \lambda_i^{\text{RU}} \quad \forall i \in \Omega_{\text{chp}} \tag{12}$$

3) Objective Function and Operational Restriction Indices: Operational restriction indices λ^{PMAX}, λ^{PMIN}, λ^{RU}, λ^{RD} are defined to indicate system bottlenecks on generation capacity, downward power adjustment margin (flexible start-up and shut-down), upward ramp rate limit and downward ramp rate limit, respectively. The detailed formulations are presented in (13).

$$\begin{aligned} \lambda^{\text{PMAX}} &= \sum_{i \in \Omega_{\text{g}} \bigcup \Omega_{\text{chp}}} \lambda_i^{\text{PMAX}} \qquad \lambda^{\text{PMIN}} = \sum_{i \in \Omega_{\text{g}} \bigcup \Omega_{\text{chp}}} \lambda_i^{\text{PMIN}} \\ \lambda^{\text{RU}} &= \sum_{i \in \Omega_{\text{g}} \bigcup \Omega_{\text{chp}}} \lambda_i^{\text{RU}} \qquad \lambda^{\text{RD}} = \sum_{i \in \Omega_{\text{g}} \bigcup \Omega_{\text{chp}}} \lambda_i^{\text{RD}} \end{aligned} \tag{13}$$

In order to eliminate system bottlenecks with the minimum amount of parameters slacked, the objective function is set as the weighted average of slack variables, as shown in (14).

$$\text{obj} = \omega^{\text{PMAX}} \cdot \lambda^{\text{PMAX}} + \omega^{\text{PMIN}} \cdot \lambda^{\text{PMIN}} + \omega^{\text{RU}} \cdot \lambda^{\text{RU}} + \omega^{\text{RD}} \cdot \lambda^{\text{RD}} \tag{14}$$

As a result, if the optimal objective function is zero, the system has no bottlenecks under the given scenario, thus no investment is required to eliminate system bottlenecks; otherwise, bottlenecks can be identified by the values of operational restriction indices. Note that the operational restriction indices make sense only if an optimal solution (or optimal solution within an acceptable tolerance) of the optimization problem is found. In addition, the existence of system operational bottleneck can be ensured if the lower bound of the objective function is greater than zero.

B. Feasibility Analysis

One may concern whether the proposed relaxed formulation is always feasible under given renewable generation and load profiles, especially for some extreme renewable generation scenarios that we are interested in. The following proposition can ensure the feasibility of the proposed formulation. Thus, the formulation can be used to conduct operational bottleneck identification analysis with a large number of scenarios.

For any given value of load power profile $D_{i,t}$, renewable power profile $W_{i,t}$ and system setting, if conditions (15)-(16) are satisfied, constraints (1)-(12) always form a feasible region.

$$\sum_{i\in\Omega_{\rm d}} D_{i,t} - \sum_{i\in\Omega_{\rm w}} W_{i,t} \geq 0 \quad \forall t \tag{15}$$

$$\prod_{i\in\Omega_{\rm g}} L_i = 0 \tag{16}$$

The idea of the proof is to find a special feasible solution satisfying constraints (1)-(12). Set the values of binary variables as (17)-(18), and the value of $\lambda_i^{\rm PMIN}$ as its maximum value in (19) to achieve the maximum flexibility in downward adjustment. It can be verified that the values of binary variables satisfy (2)-(3) and (7)-(8).

$$\tilde{u}_{i,t} = \begin{cases} 0 & \text{if } L_i \geq 1,\ t \in [1, L_i] \\ 1 & \text{otherwise} \end{cases} \quad \forall i \in \Omega_{\rm g}, t \tag{17}$$

$$\tilde{v}_{i,t} = \max\left\{\tilde{u}_{i,t} - \tilde{u}_{i,t-1}, 0\right\}, \tilde{w}_{i,t} = \max\left\{\tilde{u}_{i,t-1} - \tilde{u}_{i,t}, 0\right\} \quad \forall i \in \Omega_{\rm g}, t \tag{18}$$

$$\tilde{\lambda}_i^{\rm PMIN} = \begin{cases} \underline{P}_i \tilde{u}_{i,t} & \text{if } \forall i \in \Omega_{\rm g} \\ \max\left\{\underline{P}_i - c_i^{\rm v2} h_{i,t},\ c_i^{\rm m} h_{i,t} + \phi_i\right\} & \text{if } \forall i \in \Omega_{\rm chp} \end{cases} \tag{19}$$

Under (17)-(19), equation (20) is equivalent to (6).

$$p_{i,t} = \hat{p}_{i,t} \quad \forall i \in \Omega_{\rm g}, t \tag{20}$$

Applying equations (19)-(20) to (4), (5), (1), (9) and (12), we can get (21)-(25).

$$0 \leq p_{i,t} \leq \overline{P}_{i,t}^{*} + \tilde{u}_{i,t}\lambda_i^{\rm PMAX} \quad \forall i \in \Omega_{\rm g}, t \tag{21}$$

$$0 \leq p_{i,t} \leq \overline{P}_{i,t}^{*} + \lambda_i^{\rm PMAX} \quad \forall i \in \Omega_{\rm chp}, t \tag{22}$$

$$-\left(RD_i + \lambda_i^{\rm RD}\right)\cdot\Delta t \leq p_{i,t+1} - p_{i,t} \leq \left(RU_i + \lambda_i^{\rm RU}\right)\cdot\Delta t \quad \forall i \in \Omega_{\rm g}\bigcup\Omega_{\rm chp}, t \in [1, N_t - 1] \tag{23}$$

$$\sum_{i\in\Omega_{\rm g}\bigcup\Omega_{\rm chp}} p_{i,t} = \sum_{i\in\Omega_{\rm d}} D_{i,t} - \sum_{i\in\Omega_{\rm w}} W_{i,t} \quad \forall t \tag{24}$$

$$0 \leq \lambda_i^{\rm PMAX},\ 0 \leq \lambda_i^{\rm RD},\ 0 \leq \lambda_i^{\rm RU} \quad \forall i \in \Omega_{\rm g}\bigcup\Omega_{\rm chp} \tag{25}$$

with,

$$\overline{P}_{i,t}^{*} = \begin{cases} \overline{P}_i \tilde{u}_{i,t} & \text{if } \forall i \in \Omega_{\rm g} \\ \overline{P}_i - c_i^{\rm v1} h_{i,t} & \text{if } \forall i \in \Omega_{\rm chp} \end{cases} \quad \forall t \tag{26}$$

A feasible solution of constraints (21)-(25) can be found under conditions (15)-(16), as shown in (27)-(30).

$$\tilde{\hat{p}}_{i,t} = \tilde{p}_{i,t} = \frac{\overline{P}_{i,t}^{*}}{\sum_{i\in\Omega_{\rm g}\bigcup\Omega_{\rm chp}} \overline{P}_{i,t}^{*}} \cdot \left(\sum_{i\in\Omega_{\rm d}} D_{i,t} - \sum_{i\in\Omega_{\rm w}} W_{i,t}\right) \quad \forall i \in \Omega_{\rm g}\bigcup\Omega_{\rm chp}, t \tag{27}$$

$$\tilde{\lambda}_i^{\rm PMAX} = \max_t \left\{\left[\tilde{p}_{i,t} - \overline{P}_{i,t}^{*}\right]^{+}\right\} \quad \forall i \in \Omega_{\rm g}\bigcup\Omega_{\rm chp} \tag{28}$$

$$\tilde{\lambda}_i^{\rm RU} = \max_{t\in[1,N_t-1]} \left\{\left[\left(\tilde{p}_{i,t+1} - \tilde{p}_{i,t}\right)/\Delta t - RU_i\right]^{+}\right\} \quad \forall i \in \Omega_{\rm g}\bigcup\Omega_{\rm chp} \tag{29}$$

$$\tilde{\lambda}_i^{\rm RD} = \max_{t\in[1,N_t-1]} \left\{\left[\left(\tilde{p}_{i,t} - \tilde{p}_{i,t+1}\right)/\Delta t - RD_i\right]^{+}\right\} \quad \forall i \in \Omega_{\rm g}\bigcup\Omega_{\rm chp} \tag{30}$$

Thus, equations (17)-(19) and (27)-(30) form a feasible solution for constraints (1)-(12) under conditions (15)-(16).

In fact, the condition (15) ensures the renewable power is not greater than the load power, which is usually valid in current power systems. In the case of very high renewable energy penetration where condition (15) is not satisfied, an extended approach is presented in section IV-C. Condition (16) guarantees at least one unit is online for each time slot, so that the denominator of (27) is nonzero. Practically, the system load is usually positive, which requires at least one unit online. Thus, condition (16) satisfies in general cases.

C. Linearized Formulation

Due to the presence of nonlinear product terms and piecewise functions in (4) and (6), the optimization problem is a mixed-integer nonlinear programming (MINLP). It is computationally expensive, and difficult to be handled by most commercial solvers. Linearization of (4) and (6) is presented in this subsection to convert the formulation to an MILP.

1) Linearization of Equation (4): The product term of a nonnegative continuous variable and a binary variable can be eliminated by linearization techniques in [23]. By defining $\gamma_{i,t}^{\rm PMAX}$ in (31), the equivalence between (31) and (32)-(33) can be achieved.

$$\gamma_{i,t}^{\rm PMAX} \overset{\rm def}{=} \lambda_i^{\rm PMAX} u_{i,t} \tag{31}$$

$$\underline{\lambda}_i^{\rm PMAX} u_{i,t} \leq \gamma_{i,t}^{\rm PMAX} \leq \overline{\lambda}_i^{\rm PMAX} u_{i,t} \tag{32}$$

$$\overline{\lambda}_i^{\rm PMAX}\left(u_{i,t} - 1\right) \leq \gamma_{i,t}^{\rm PMAX} - \lambda_i^{\rm PMAX} \leq \underline{\lambda}_i^{\rm PMAX}\left(u_{i,t} - 1\right) \tag{33}$$

Analogously, by defining $\gamma_{i,t}^{\rm PMIN}$ in (34), the equivalence between (34) and (35)-(36) can be obtained.

$$\gamma_{i,t}^{\rm PMIN} \overset{\rm def}{=} \lambda_i^{\rm PMIN} u_{i,t} \tag{34}$$

$$\underline{\lambda}_i^{\rm PMIN} u_{i,t} \leq \gamma_{i,t}^{\rm PMIN} \leq \overline{\lambda}_i^{\rm PMIN} u_{i,t} \tag{35}$$

$$\overline{\lambda}_i^{\rm PMIN}\left(u_{i,s,t} - 1\right) \leq \gamma_{i,t}^{\rm PMIN} - \lambda_i^{\rm PMIN} \leq \underline{\lambda}_i^{\rm PMIN}\left(u_{i,s,t} - 1\right) \tag{36}$$

Then, equation (4) can be replaced by (37), (32)-(33) and (35)-(36).

$$0 \le \hat{p}_{i,t} \le \left(\overline{P}_i - \underline{P}_i\right) u_{i,t} + \gamma_{i,t}^{\text{PMAX}} + \gamma_{i,t}^{\text{PMIN}} \quad \forall i \in \Omega_{\text{g}}, t \tag{37}$$

2) Linearization of Equation (6): The productive term $\lambda_i^{\text{PMIN}} u_{i,t}$ in (6) can be easily replaced by $\gamma_{i,t}^{\text{PMIN}}$ using the definition in (34). The linearization of piecewise functions and their product terms with binary variables is then addressed.

$$\begin{aligned}
&\left[RU_i^{\text{SU}} \cdot \Delta t \cdot l - \lambda_i^{\text{PMIN}}\right]^+ \cdot v_{i,t+T_i^{\text{DSU}}-l+1} \\
&\overset{\text{(a)}}{=} \left[RU_i^{\text{SU}} \cdot \Delta t \cdot l \cdot v_{i,t+T_i^{\text{DSU}}-l+1} - \lambda_i^{\text{PMIN}} \cdot v_{i,t+T_i^{\text{DSU}}-l+1}\right]^+ \\
&\overset{\text{(b)}}{=} \left[RU_i^{\text{SU}} \cdot \Delta t \cdot l \cdot v_{i,t+T_i^{\text{DSU}}-l+1} - \lambda_i^{\text{PMIN}}\right]^+
\end{aligned} \tag{38}$$

The LHS of (38) is simplified to a piecewise linear function without product terms. Because $v_{i,t+T_i^{\text{DSU}}-l+1}$ is a binary variable, the equivalence of (a) can be checked with both 0 and 1 value of $v_{i,t+T_i^{\text{DSU}}-l+1}$. The equivalence of (b) takes advantage of the binary variable $v_{i,t+T_i^{\text{DSU}}-l+1}$ and the fact $\lambda_i^{\text{PMIN}} \ge 0$. It is trivially valid when $v_{i,t+T_i^{\text{DSU}}-l+1} = 1$, and RHS $= [-\lambda_i^{\text{PMIN}}]^+ = 0 =$ LHS when $v_{i,t+T_i^{\text{DSU}}-l+1} = 0$.

By defining $\xi_{i,t,l}^{\text{SU}+}$ in (39), the equivalence of (39) and (40)-(42) can be derived given the bound of $RU_i^{\text{SU}} \cdot \Delta t \cdot l \cdot v_{i,t+T_i^{\text{DSU}}-l+1} - \lambda_i^{\text{PMIN}}$ as shown in (43),

$$\xi_{i,t,l}^{\text{SU}+} \overset{\text{def}}{=} \left[RU_i^{\text{SU}} \cdot \Delta t \cdot l \cdot v_{i,t+T_i^{\text{DSU}}-l+1} - \lambda_i^{\text{PMIN}}\right]^+ \tag{39}$$

$$RU_i^{\text{SU}} \cdot \Delta t \cdot l \cdot v_{i,t+T_i^{\text{DSU}}-l+1} - \lambda_i^{\text{PMIN}} = \xi_{i,t,l}^{\text{SU}+} - \xi_{i,t,l}^{\text{SU}-} \tag{40}$$

$$0 \le \xi_{i,t,l}^{\text{SU}+} \le \left(RU_i^{\text{SU}} \cdot \Delta t \cdot l\right) \cdot \delta_{i,t,l}^{\text{SU}} \tag{41}$$

$$0 \le \xi_{i,t,l}^{\text{SU}-} \le \underline{P}_i \cdot \left(1 - \delta_{i,t,l}^{\text{SU}}\right) \tag{42}$$

$$RU_i^{\text{SU}} \cdot \Delta t \cdot l \cdot v_{i,t+T_i^{\text{DSU}}-l+1} - \lambda_i^{\text{PMIN}} \in \left[-\underline{P}_i, RU_i^{\text{SU}} \cdot \Delta t \cdot l\right] \tag{43}$$

Analogously, by defining $\xi_{i,t,l}^{\text{SD}+}$ in (44), the equivalence of (44) and (45)-(47) can be obtained.

$$\xi_{i,t,l}^{\text{SD}+} \overset{\text{def}}{=} \left[\left(\underline{P}_i - RD_i^{\text{SD}} \cdot \Delta t \cdot (l-1)\right) \cdot w_{i,t-l+1} - \lambda_i^{\text{PMIN}}\right]^+ \tag{44}$$

$$\left(\underline{P}_i - RD_i^{\text{SD}} \cdot \Delta t \cdot (l-1)\right) \cdot w_{i,t-l+1} - \lambda_i^{\text{PMIN}} = \xi_{i,t,l}^{\text{SD}+} - \xi_{i,t,l}^{\text{SD}-} \tag{45}$$

$$0 \le \xi_{i,t,l}^{\text{SD}+} \le \left(\underline{P}_i - RD_i^{\text{SD}} \cdot \Delta t \cdot (l-1)\right) \cdot \delta_{i,t,l}^{\text{SD}} \tag{46}$$

$$0 \le \xi_{i,t,l}^{\text{SD}-} \le \underline{P}_i \cdot \left(1 - \delta_{i,t,l}^{\text{SD}}\right) \tag{47}$$

Finally, equation (6) can be replaced by (48), (40)-(42) and (45)-(47).

$$p_{i,t} = \hat{p}_{i,t} + \underline{P}_i u_{i,t} - \gamma_{i,t}^{\text{PMIN}} + \sum_{l=1}^{T_i^{\text{DSU}}} \xi_{i,t,l}^{\text{SU}+} + \sum_{l=1}^{T_i^{\text{DSD}}} \xi_{i,t,l}^{\text{SD}+} \quad \forall i \in \Omega_{\text{g}}, t \tag{48}$$

In addition, if a start-up trajectory is non-decreasing, the binary indicator $\delta_{i,t,l}^{\text{SU}}$ for points in one trajectory should be non-decreasing, which is expressed in (49). Analogously, if a shut-down trajectory is non-increasing, the non-increasing $\delta_{i,t,l}^{\text{SD}}$ is expressed in (50).

$$\begin{aligned}
&\delta_{i,t_1,l_1}^{\text{SU}} \le \delta_{i,t_2,l_2}^{\text{SU}} \\
&\quad \forall i \in \Omega_{\text{g}}, (t_1, l_1, t_2, l_2) \in \{t_1 + l_1 = t_2 + l_2, l_1 \le l_2\}
\end{aligned} \tag{49}$$

$$\begin{aligned}
&\delta_{i,t_1,l_1}^{\text{SD}} \ge \delta_{i,t_2,l_2}^{\text{SD}} \\
&\quad \forall i \in \Omega_{\text{g}}, (t_1, l_1, t_2, l_2) \in \{t_1 + l_1 = t_2 + l_2, l_1 \le l_2\}
\end{aligned} \tag{50}$$

The binary indicators $\delta_{i,t,l}^{\text{SU}}$ or $\delta_{i,t,l}^{\text{SD}}$ for a trajectory should be zero if the corresponding start-up or shut-down status variables $v_{i,t}$ or $w_{i,t}$ is zero, as shown in (51) and (52) respectively.

$$\delta_{i,t,T_i^{\text{DSU}}}^{\text{SU}} \le v_{i,t+1} \quad \forall i \in \Omega_{\text{g}}, t \in [1, N_t - 1] \tag{51}$$

$$\delta_{i,t,1}^{\text{SD}} \le w_{i,t} \quad \forall i \in \Omega_{\text{g}}, t \in [1, N_t] \tag{52}$$

Equations (49)-(52) can be added to reduce the computational time if their sizes are appropriate in a specific problem.

3) MILP Formulation: Finally, an MILP formulation for system operational bottleneck identification is established to find operational bottlenecks in the scope of system balance. The detailed formulation is demonstrated in (53).

$$\begin{aligned}
\min \quad & \text{Equation (14)} \\
\text{s.t.} \quad & \text{Equations (1)-(3), (5), (7)-(12), (32)-(33), (35)-(37),} \\
& \text{(40)-(42), (45)-(48).} \\
& \text{Equations (49)-(52), if necessary.}
\end{aligned} \tag{53}$$

III. DBSCAN Based Scenario Clustering

In order to conduct cost-effectiveness comparisons for energy storage under different bottleneck types, all the scenarios under which system bottleneck exists, are clustered according to their corresponding operational restriction indices. The most commonly used clustering method is the k-means clustering algorithm. It can be easily implemented and performs well in numerous applications. However, the main drawback of extending this method to our current work, is the number of clusters k should be pre-specified. It is not applicable to operational restrictive indices based scenario clustering, because one cannot identify how many types of bottlenecks will occur before investigating a system. Density-based spatial clustering of applications with noise (DBSCAN) is a clustering algorithm with the advantage of auto-deciding the number of clusters based on the density metric [24]. If there are a small number of scenarios that lead to different system bottlenecks with the majority, they will be recognized as noises in the algorithm. Then we can investigate them independently. The detailed implementation of DBSCAN can be referred to [24].

In this work, each operational restriction index is defined to measure a type of bottleneck, i.e., the bottleneck on generation capacity, downward power adjustment margin (flexible start-up and shut-down), upward ramp rate limit and downward ramp rate limit. Therefore, an appropriate metric is required to define the similarity of scenarios. The most commonly used Euclidean distance might fail in measuring the typological difference of some scenarios in our clustering application.

For demonstration simplicity, operational restriction indices are expressed as a vector form in (54).

$$\lambda = \left[\lambda^{\text{PMAX}},\ \lambda^{\text{PMIN}},\ \lambda^{\text{RU}},\ \lambda^{\text{RD}}\right]^\top \tag{54}$$

For example, let $\lambda_1 = [1,0,0,0]^\top$ for scenario 1, which means the system lacks generation capacity by 1 unit. For scenario 2, $\lambda_2 = [10,0,0,0]^\top$ indicates the system is short of generation capacity by 10 units. While for scenario 3, $\lambda_3 = [0,0,1,0]^\top$ shows the system exists bottleneck on the upward ramp rate by 1 unit. As a result, although scenarios 1 and 2 lead to the same type of system bottlenecks, the distance of λ_1 and λ_2 is 9, which is farther than the distance of λ_1 and λ_3, $\sqrt{2}$.

Thus, in order to calculate the similarity of scenarios according to the operational restriction indices, the cosine similarity metric is used in this work. The similarity metric is defined in (55), then the distance used in the clustering algorithm is defined in (56). In the aforementioned case, the distance of λ_1 and λ_2 is 0, while the distance of λ_1 and λ_3 is 1. The defined distance can appropriately quantify the typological difference of bottlenecks for any two given scenarios.

$$\begin{aligned}\text{siml}_{s1,s2} &= \frac{\lambda_{s1}\cdot\lambda_{s2}}{\|\lambda_{s1}\|\,\|\lambda_{s2}\|} \\ &= \frac{\sum_{*=\text{PMAX,PMIN,RU,RD}} \lambda^*_{s1}\lambda^*_{s2}}{\sqrt{\sum_{*=\text{PMAX,PMIN,RU,RD}} {\lambda^*_{s1}}^2}\sqrt{\sum_{*=\text{PMAX,PMIN,RU,RD}} {\lambda^*_{s2}}^2}}\end{aligned} \tag{55}$$

$$\text{dist}_{s1,s2} = 1 - \text{siml}_{s1,s2} \tag{56}$$

IV. Framework

A. Framework Description

The proposed approach aims to define, identify and eliminate system operational bottlenecks in the scope of system balance. It includes steps of operational bottleneck identification, cosine similarity based DBSCAN and cost-effectiveness comparative analysis. A final conclusion on the cost-effectiveness of energy storage investment in bottleneck elimination is made, through the establishment of connections between cluster characteristics and bottleneck elimination options.

A bottleneck identification approach is conducted firstly to quantify system operational bottlenecks in various aspects from the perspective of system balance, i.e., generation capacity, downward power adjustment margin (flexible start-up and shut-down), upward ramp rate limit and downward ramp rate limit. Quantitative measures of bottlenecks in each scenario are defined by operational restriction indices. Then these scenarios are distributed into one or more clusters by cosine similarity based DBSCAN according to their corresponding bottleneck characteristics. Finally, various bottleneck elimination options, including energy storage with different technologies, are compared for each cluster. A comparative analysis on cost-effectiveness is conducted to draw the conclusion of this work.

The flowchart of the proposed approach is shown in Fig. 1. The inputs of this process consist of data for system components, system structure, renewable generation profiles and load profiles. The outputs include system bottlenecks found within each cluster, and conclusions on the cost-effectiveness of energy storage investment in bottleneck elimination. The proposed approach can also be used to analyze the pros and cons of elimination options with different technologies.

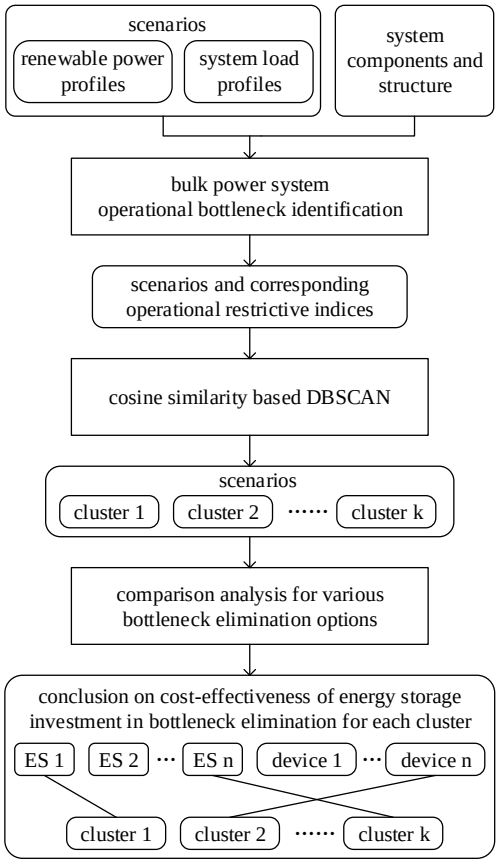

Fig. 1. Flowchart of the proposed approach.

B. Cost-Effectiveness Comparison for Elimination Options

After conducting cosine similarity based DBSCAN, scenarios are attributed to one or more clusters according to their bottleneck types. The further analysis aims to investigate relations between cluster features and the cost-effectiveness of energy storage investment. Then operational bottleneck types with strong requirements on energy storage investment can be found. The analysis can not only give insight on how energy storage should be utilized to eliminate system bottlenecks, but also provide investment suggestions for a specific power system with certain types of bottlenecks.

Given various technological options that are able to contribute to bottleneck elimination, and their current construction costs, investment optimizations are performed for each scenario and each option. Then the corresponding minimum costs for system bottleneck elimination can be obtained. A match analysis of clusters and elimination options is then performed, to establish relations between bottleneck features and the cost-effectiveness of options. In this paper, technological options include battery storages with different technologies, pumped

storage, compressed air energy storage, thermal storage, and conventional generator, depending on the particular system. Detailed investment optimization models are referred to [11], [22] and [25].

C. Extensions

Our approach can be flexibly extended for higher renewable energy penetrated systems, or transmission line congested systems.

1) For Higher Renewable Energy Penetration Levels: The proposed bottleneck identification model has a sufficient solvability condition (15), which potentially limits the penetration of renewable energy. With the expectation that a higher share of renewable energy will appear in further power systems, our approach can be extended to address this issue.

When (15) is not satisfied, note the system balance cannot be achieved even all the conventional generators shut down. To this end, we defined an additional operation restriction index λ^{MAXRO} to measure the maximum power that renewable generation exceeds load, as indicated in (57). This index corresponds to renewable energy over-generation bottlenecks. In fact, λ^{MAXRO} is a complementary index for operation restriction index λ^{PMIN} when λ^{PMIN} reaches its upper limit, as λ_i^{PMIN} for each generator cannot be greater than $\underline{P}_i$ (otherwise negative generation might occur for generators, which goes against common sense).

$$\lambda^{\text{MAXRO}} = \max\left\{\max_t\left(\sum_{i\in\Omega_{\text{w}}} W_{i,t} - \sum_{i\in\Omega_{\text{d}}} D_{i,t}\right),\ 0\right\} \quad (57)$$

For the bottleneck identification model, the operation restriction index λ^{MAXRO} is first calculated using (57), then (58) is used to replace the power balance constraint (1) when condition (15) is not satisfied for high renewable energy penetration cases.

$$\sum_{i\in\Omega_{\text{g}}\bigcup\Omega_{\text{chp}}} p_{i,t} = \max\left\{\sum_{i\in\Omega_{\text{d}}} D_{i,t} - \sum_{i\in\Omega_{\text{w}}} W_{i,t},\ 0\right\} \quad \forall t \quad (58)$$

For the DBSCAN based scenario clustering, a general downward power adjustment operation restriction index λ^{PMING}, which is the sum of λ^{PMIN} and λ^{MAXRO} as defined in (59), is used to replace λ^{PMIN} in (55).

$$\lambda^{\text{PMING}} = \lambda^{\text{PMIN}} + \lambda^{\text{MAXRO}} \quad (59)$$

2) For Congestion Bottlenecks: Following the current industrial practice of power system planning, which performs generation expansion planning and transmission expansion planning in a two-stage framework, the proposed approach can also be extended to address congestion bottlenecks in a two-stage manner. Detailed investigations are beyond the scope of this paper. A related research indicates energy storage investment is more economical versus transmission line investment when the transmission distance is relatively long [26].

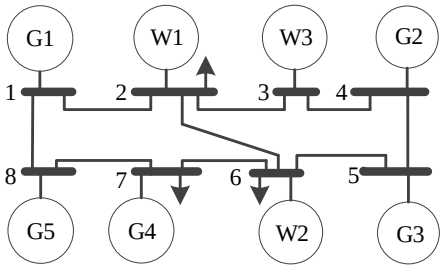

Fig. 2. Diagram of modified 8-bus power system.

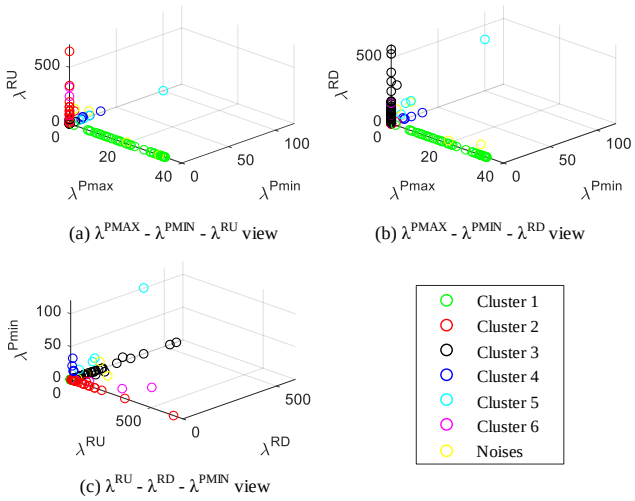

(a) λ^{PMAX} - λ^{PMIN} - λ^{RU} view (b) λ^{PMAX} - λ^{PMIN} - λ^{RD} view

(c) λ^{RU} - λ^{RD} - λ^{PMIN} view

Fig. 3. Clustering results of the 8-bus test system.

V. Case Study

An 8-bus test system and a practical northeast China provincial power system were used to illustrate the proposed system operational bottleneck identification and elimination method. All the MILP problems were solved by CPLEX 12.8 [27] on a computer with dual Intel Xeon CPU E5-2650 and 128 GB RAM. The gap tolerance was set as 0.01%.

A. 8-Bus Test System

The 8-bus test system aims to provide analyses on system bottlenecks as much as possible, in order to provide some insights on the most economical technical option for each scenario cluster.

1) System Setting: The 8-bus test system contains five generators and two wind farms. The overall capacities of generators and wind farms are 3500 MW and 1900 MW, respectively. The wind power data that contains 2190 daily scenarios, is scaled from NREL Wind Integration Data Sets [28]. The diagram of 8-bus test system is presented in Fig. 2. In order to reflect wind ramp characters in minute-scale, dispatch interval is set as 15 min, and unit commitment interval was set as 1 hour. Formulations presented above can be easily extended without loss of generality.

2) Analysis Results: Among the total 2190 scenarios, 140 daily scenarios that will cause system bottlenecks are found, after conducting system operational bottleneck identification.

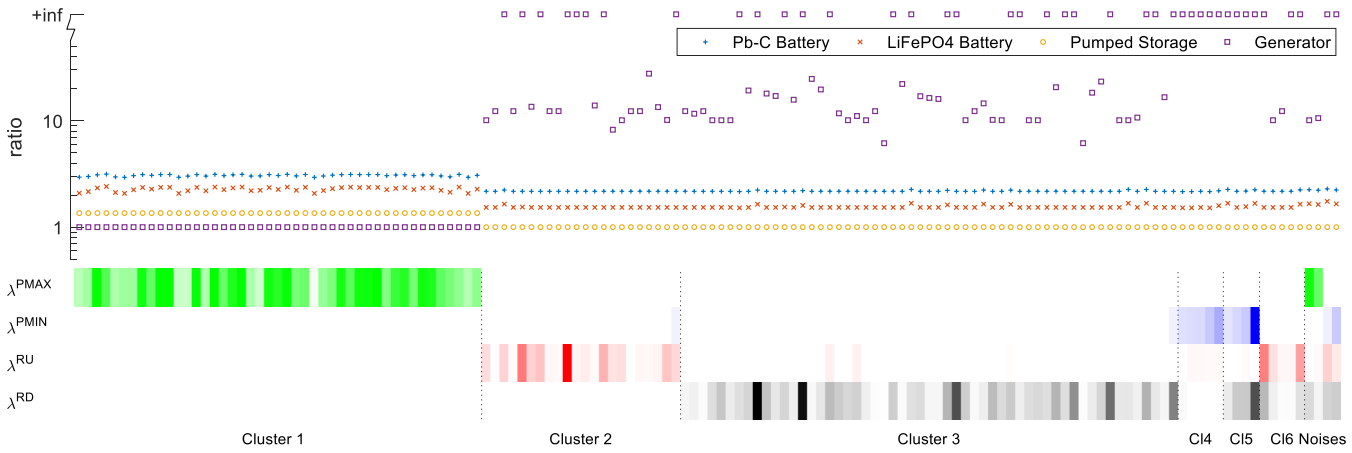

Fig. 4. Cost-effectiveness comparison results.

As shown in Fig. 3, the 140 scenarios are then clustered into 6 groups by performing the cosine similarity based DBSCAN. As indicated, the main system bottlenecks caused by scenarios in cluster 1 is overload, i.e., lacking system generation capacity. Scenarios in clusters 2 and 3 mostly lead to insufficient power upward and downward ramp ability, respectively. Scenarios in cluster 4 mainly result in power downward adjustment bottlenecks, as well as flexible start-up and shut-down bottlenecks in more severe cases. Bottlenecks identified in cluster 5 are combinations of inadequate power downward adjustment and downward ramp abilities. Bottlenecks in cluster 6 are mainly induced by upward and downward ramp events. Noises are combinations of the aforementioned factors, which are far from other scenarios.

The minimum investment required to eliminate system bottlenecks for each scenario is then calculated for Pb-C battery, $LiFeO_4$ battery, pumped storage and generator. The cost-effectiveness comparisons for each cluster and each technological option are shown in Fig. 4. The color map visualizes normalized values of system restriction indices, in which deeper color corresponds to a larger value in each line. Investment ratio is defined in (60) for a clearer comparison, in which $\mathrm{Inv}_{s,k}$ denotes investment cost for bottleneck elimination in scenarios s with technological option k.

$$\mathrm{ratio}_{s,k} = \mathrm{Inv}_{s,k} \Big/ \min_{k} \mathrm{Inv}_{s,k} \quad \forall s,k \tag{60}$$

It can be found that investments of energy storage are much less than investments of generators for cluster 2-6, in which there even exists some scenarios that generator investments are unable to eliminate bottlenecks. Fig. 4 also shows, if natural conditions allowed, pumped storage is the best choice under current prices. On the other side, results of cluster 1 indicate generator is a better option for generation capacity inadequacy.

B. Northeast China Provincial Power System

A northeast China provincial power grid is used to verify the effectiveness of the proposed method in a real-world system.

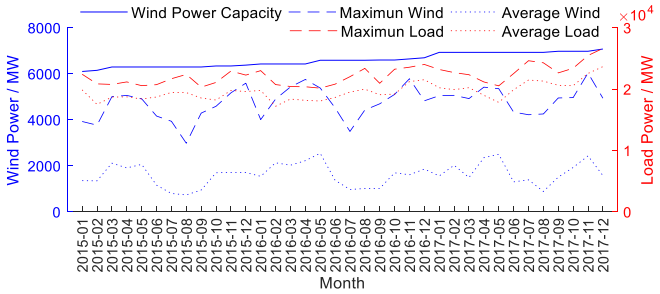

Fig. 5. Monthly statistics of wind and load profiles.

1) System Setting: The system consists of 105 conventional generators with 33268.5 MW total capacity. In this region, as the coal-fired central heating system works from early November to late March of the next year, 51 and 60 units operate at CHP mode during initial-and-terminal months (November and March) and intermediate months (December, January, and February) respectively. The overall capacity of wind farms is constantly increasing in recent years from 6103 MW to 7079 MW, as shown in Fig. 5. Monthly statistics of wind and load profiles are also presented in Fig. 5, which indicates wind power fluctuates heavily because its average curve is far from its maximum curve. Real hourly wind power and load data is used, which contains 1096 daily scenarios from the year 2015 to 2017. In operational bottleneck identification and investment problems, dispatch and unit commitment intervals are both set as 1 hour.

2) Analysis Results for Past Scenarios: Among total of 1096 scenarios, 161 scenarios that cause system operational bottlenecks are recognized. After performing cosine similarity based DBSCAN, the 161 scenarios are all attributed to one cluster. As indicated in Fig. 6, power downward adjustment ability is the main bottleneck for scenarios in the cluster. In this case, cosine similarity based DBSCAN was verified well-working without a pre-specify number of clusters, even when all the system operational bottlenecks belong to the same category.

The distribution of the 161 scenarios during the whole year

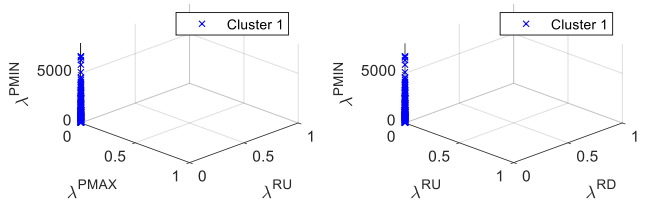

(a) λ^{PMAX} - λ^{RU} - λ^{PMIN} view (b) λ^{RU} - λ^{RD} - λ^{PMIN} view

Fig. 6. Clustering results of northeast China provincial power system.

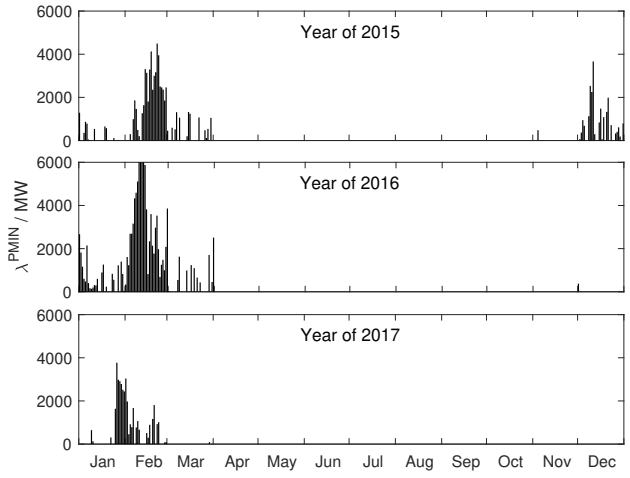

Fig. 7. Distribution of bottlenecks in each year.

is shown in Fig. 7, from the year 2015 to 2017. As indicated, almost all daily scenarios with operational bottlenecks appear during the heating season, i.e., November to March of the next year. The majority of the most severe system operational bottlenecks happen during the intermediate months of the heating season, i.e., December to February of the next year.

Minimum investment costs to eliminate bottlenecks using Pb-C battery, $LiFeO_4$ battery, pumped storage, compressed air energy storage, thermal storage, and generator are calculated. Fig. 8 presents cost-effectiveness comparisons between different elimination options, indicating that thermal storage is the most economical device to eliminate operational bottlenecks that occur in this system.

3) Analysis Results for Future Scenarios: The penetration of renewable energy sources in the aforementioned case ranges from 15.5% to 17.5% due to the continuing wind farm installations. In order to test the proposed method, we increase the penetration level to ∼50% (ranges from 48.3% to 52.0%).

As the wind power exceeds the load in some scenarios, we conducted the extended approach in section IV-C. All the 654 scenarios among the total of 1096 scenarios also belong to one cluster according to the results of DBSCAN based scenario clustering. In this cluster, the main bottleneck is also power downward adjustment ability and/or renewable energy over-generation. Cost-effectiveness analyses were conducted for two groups: one contains scenarios in the heating season; another contains scenarios in the non-heating season. For heating season scenarios, conclusions are similar to the past case, as shown in Fig. 9. However, for non-heating season scenarios, as indicated in Fig. 10, pumped storage and compressed air energy storage are the most economical options for bottleneck elimination if natural conditions allow. The reason is heat load is not enough to make use of the energy stored in heat storage for non-heating season scenarios, which makes heat storage unable to address the system bottlenecks. We note the compressed air energy storage has similar performance with pumped storage in cost-effectiveness. Due to the rigid requirements on natural conditions for pumped storage installation, compressed air energy storage has vast potentials to eliminate system bottlenecks economically.

VI. Conclusion

This paper presented an approach to define, identify and eliminate operational bottlenecks in the scope of system balance for renewable energy integrated bulk power systems. An MILP formulation for system bottleneck identification was proposed first to identify system operational bottlenecks. Operational restriction indices were defined to quantify such bottlenecks. The cosine similarity based DBSCAN algorithm was then used in operational restriction indices based scenario clustering. Finally, the cost-effectiveness comparative analysis was conducted for various elimination options, including energy storage with different technologies. An 8-bus test system and a practical northeast China provincial power system were used to verify the proposed approach. Power ramp limits (including upward and downward ramps) and power downward adjustment dominated bottlenecks were found to be strongly required for energy storage elimination. Thermal and pumped storages are better options if natural conditions satisfy. However, the generator is a better choice for generation capacity dominated bottlenecks under current price.

Acknowledgment

The authors would like to thank Mr. Weiyu Chen for the useful discussion on clustering methods.

References

[1] S. Killinger, N. Kreifels, B. Burger, B. Müller, G. Stiff, and C. Wittwer, "Impact of the solar eclipse from 20th March 2015 on the German electrical supply-simulation and analysis," *Energy Technol.*, vol. 4, no. 2, pp. 288–297, 2016.

[2] E. Ela and B. Kirby, "ERCOT event on February 26, 2008: lessons learned," Tech. Rep., National Renewable Energy Laboratory, 2008.

[3] J. Freedman and M. Markus, "Analysis of west Texas wind plant ramp-up and ramp-down events," AWS Truewind, LLC, 2008.

[4] P. Sørensen and P. Pinson, "Power fluctuations from large wind farms - final report," Risø Report Risø-R-1711(EN), 2009.

[5] N. Yan, Z. X. Xing, W. Li, and B. Zhang, "Economic dispatch application of power system with energy storage systems," *IEEE Trans. Appl. Supercond.*, vol. 26, no. 7, pp. 1-5, Oct. 2016.

[6] S. A. Abdelrazek and S. Kamalasadan, "Integrated PV capacity firming and energy time shift battery energy storage management using energy-oriented optimization," *IEEE Trans. on Ind. Applicat.*, vol. 52, no. 3, pp. 2607-2617, Feb. 2016.

[7] J. Dong, F. Gao, X. Guan, Q. Zhai, and J. Wu, "Storage sizing with peak-shaving policy for wind farm based on cyclic Markov chain model," *IEEE Trans. Sustain. Energy*, vol. 8, no. 3, pp. 978-989, Jul. 2017.

[8] Y. Gong, Q. Jiang and R. Baldick, "Ramp event forecast based wind power ramp control with energy storage system," *IEEE Trans. Power Syst.*, vol. 31, no. 3, pp. 1831-1844, May 2016.

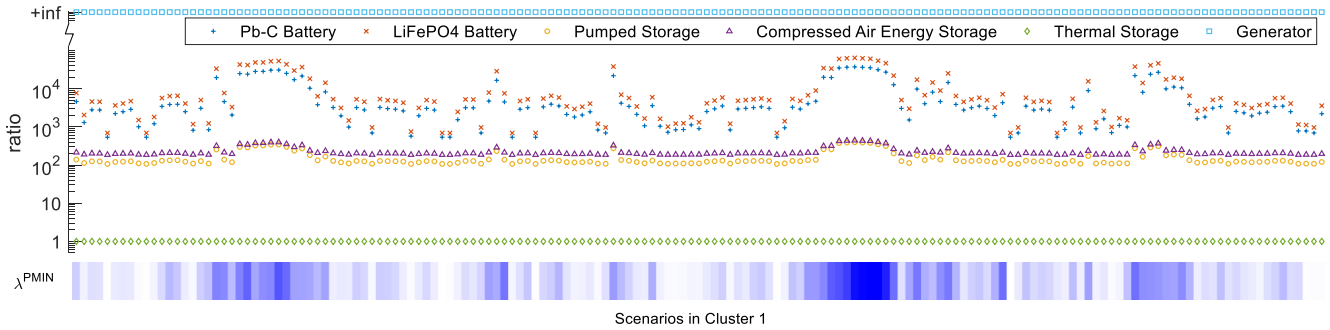

Fig. 8. Cost-effectiveness comparison results (past scenarios).

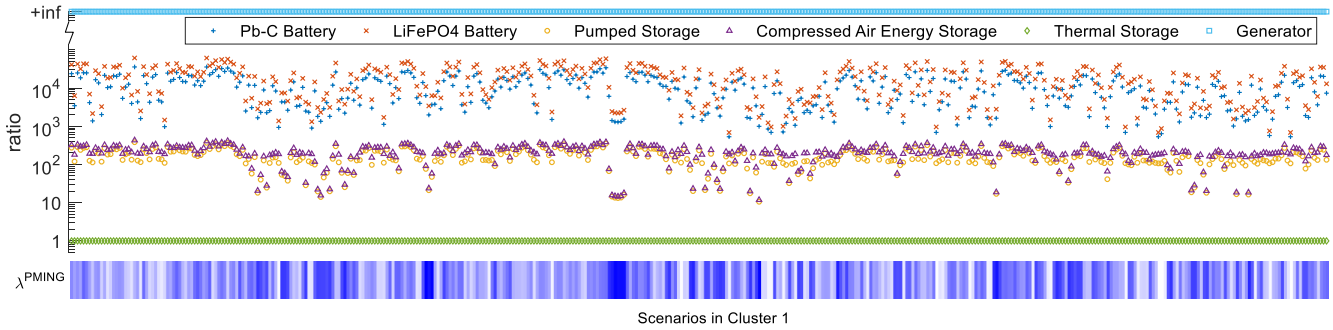

Fig. 9. Cost-effectiveness comparison results (future scenarios, heating season).

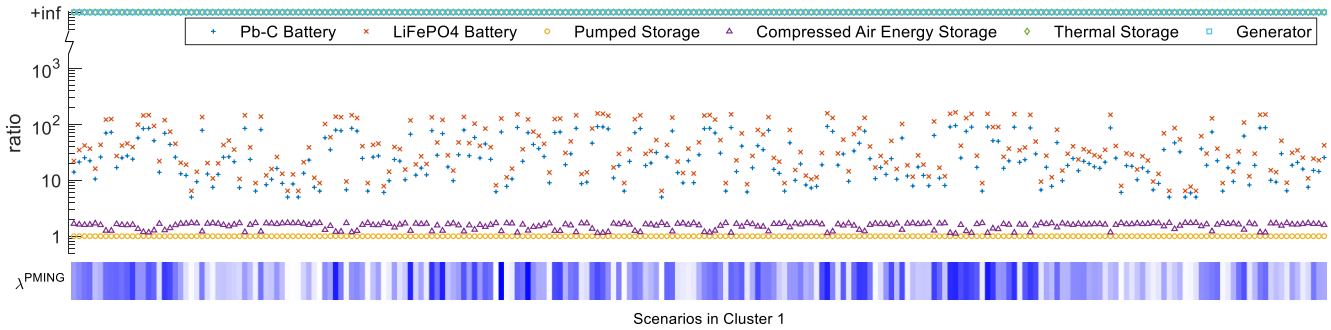

Fig. 10. Cost-effectiveness comparison results (future scenarios, non-heating season).

[9] Q. Jiang and H. Wang, "Two-time-scale coordination control for a battery energy storage system to mitigate wind power fluctuations," *IEEE Trans. Energy Convers.*, vol. 28, no. 1, pp. 52-61, Mar. 2013.

[10] K. Bruninx, Y. Dvorkin, E. Delarue, H. Pandzic, W. Dhaeseleer, and D. S. Kirschen, "Coupling pumped hydro energy storage with unit commitment," *IEEE Trans. Sustain. Energy*, vol. 7, no. 2, pp. 786-796, Apr. 2016.

[11] S. Wang, G. Geng, W. Liu, and Q. Jiang, "Impact of time-coupled generator formulation on energy storage sizing problem," in *2018 North American Power Symposium (NAPS)*, Fargo, ND, 2018, pp. 1-6.

[12] X. J. Ban, L. Chu, and H. Benouar, "Bottleneck identification and calibration for corridor management planning," *Transportation Research Record*, vol. 1999, no. 1, pp. 40-53, 2018.

[13] J. Long, Z. Gao, H. Ren, and A. Lian, "Urban traffic congestion propagation and bottleneck identification," *Sci. China Ser. F-Inf. Sci.*, vol. 51, no. 7, pp. 948-964, 2008.

[14] K. J. Mizgier, M. P. Jüttner and S. M. Wagner, "Bottleneck identification in supply chain networks," *International Journal of Production Research*, vol. 51, no. 5, pp. 1477-1490, 2013-01-01 2013.

[15] R. R. Tan, H. L. Lam, H. Kasivisvanathan, D. K. S. Ng, D. C. Y. Foo, M. Kamal, N. Hallaler, and J. J. Klemeš, "An algebraic approach to identifying bottlenecks in linear process models of multifunctional energy systems," *Theoretical Foundations of Chemical Engineering*, vol. 46, no. 6, pp. 642-650, 2012.

[16] L. Baringo and A. J. Conejo, "Correlated wind-power production and electric load scenarios for investment decisions," *Applied Energy*, vol. 101, pp. 475-482, 2013.

[17] Y. Zhao, L. Ye, W. Wang, H. Sun, Y. Ju, and Y. Tang, "Data-driven correction approach to refine power curve of wind farm under wind curtailment," *IEEE Trans. Sustain. Energy*, vol. 9, no. 1, pp. 95-105, Jan. 2018.

[18] M. Paramasivam, S. Dasgupta, V. Ajjarapu, and U. Vaidya, "Contingency analysis and identification of dynamic voltage control areas," *IEEE Trans. Power Syst.*, vol. 30, no. 6, pp. 2974-2983, Nov. 2015.

[19] H. Huang, L. Zhang, H. Qiao, and N. Du, "A method to determine step-shaped electricity consumption levels for residential area based on variable-density clustering," *Power System Technology*, vol. 34, no. 11, pp. 111-116, 2010.

[20] J. M. Arroyo and A. J. Conejo, "Modeling of start-up and shut-down power trajectories of thermal units," *IEEE Trans. Power Syst.*, vol. 19, no. 3, pp. 1562-1568, Aug. 2004.
[21] G. Morales-Espana, J. M. Latorre and A. Ramos, "Tight and compact MILP formulation of start-up and shut-down ramping in unit commitment," *IEEE Trans. Power Syst.*, vol. 28, no. 2, pp. 1288-1296, May 2013.
[22] Z. Cheng, G. Geng, Q. Jiang, and J. M. Guerrero, "Energy management of CHP-based microgrid with thermal storage for reducing wind curtailment," *Journal of Energy Engineering*, vol. 144, no. 6, p. 04018066, 2018.
[23] L. Fan, J. Wang, R. Jiang and Y. Guan, "Min-max regret bidding strategy for thermal generator considering price uncertainty," *IEEE Trans. Power Syst.*, vol. 29, no. 5, pp. 2169-2179, Sep. 2014.
[24] M. Ester, H. P. Kriegel, J. Sander, and X. Xu, "A density-based algorithm for discovering clusters in large spatial databases with noise," in *International Conference on Knowledge Discovery and Data Mining*, Portland, OR, 1996, pp. 226-231.
[25] S. Wang, Q. Jiang and Y. Ge, "Optimal configuration of energy storage considering wind ramping events," *Power System Technology*, vol. 42, no. 4, pp. 1093-1101, 2018.
[26] S. Wang, G. Geng and Q. Jiang, "Robust co-planning of energy storage and transmission line with mixed integer recourse," *IEEE Trans. Power Syst.*, vol. 34, no. 6, pp. 4728-4738, 2019.
[27] ILOG CPLEX Homepage, Armonk, NY, USA. [Online]. Available: https://www.ibm.com/products/ilog-cplex-optimization-studio. Accessed: 2019.
[28] NREL Wind Integration Data Sets, Golden, CO, USA [Online]. Available: https://www.nrel.gov/grid/wind-integration-data.html. Accessed: 2019.

Siyuan Wang received the B.S. and Ph.D. degrees in electrical engineering from the College of Electrical Engineering, Zhejiang University, Hangzhou, China, in 2013 and 2019, respectively.

He is currently a Postdoctoral Fellow with the Department of Electrical and Computer Engineering, Missouri University of Science and Technology (formerly University of Missouri-Rolla), Rolla, MO, USA. His research interests include power system planning and operation, renewable energy integration, and the application of energy storage technology in power systems.

Guangchao Geng (Senior Member, IEEE) received the B.S. and Ph.D. degrees in electrical engineering from the College of Electrical Engineering, Zhejiang University, Hangzhou, China, in 2009 and 2014, respectively.

From 2012 to 2013, he was a Visiting Student with the Department of Electrical and Computer Engineering, Iowa State University, Ames, IA, USA. From 2014 to 2017, he was a Postdoctoral Fellow with the College of Control Science and Engineering, Zhejiang University, Hangzhou, China, and the Department of Electrical and Computer Engineering, University of Alberta, Edmonton, AB, Canada. He is currently an Associate Professor with the College of Electrical Engineering, Zhejiang University, Hangzhou, China. His research interest includes power system stability and control, renewable energy integration, and high performance computing.

Junchao Ma received the B.S. and Ph.D. degrees in electrical engineering from the College of Electrical Engineering, Zhejiang University, Hangzhou, China, in 2012 and 2017, respectively.

He is currently with State Grid Zhejiang Electric Power Research Institute, Hangzhou, China. His research interest includes energy management of MVDC systems and power system operation.

Quanyuan Jiang (Senior Member, IEEE) received the B.S., M.S., and Ph.D. degrees in electrical engineering from the Huazhong University of Science and Technology, Wuhan, China, in 1997, 2000, and 2003, respectively.

From 2006 to 2008, he was a Visiting Associate Professor with the School of Electrical and Computer Engineering, Cornell University, Ithaca, NY, USA. He is currently a Professor with the College of Electrical Engineering, Zhejiang University, Hangzhou, China. His research interest includes power system stability and control, high performance computing, and applications of energy storage systems in power systems.

Hongyang Huang received the B.S. and Ph.D. degrees in electrical engineering from the College of Electrical Engineering, Zhejiang University, Hangzhou, China, in 2009 and 2014, respectively.

He is currently with State Grid Zhejiang Electric Power Research Institute, Hangzhou, China. His research interests include the analysis and the control of large-scale hybrid AC/DC power systems.

Boliang Lou received the B.S. degree in electrical engineering from Zhejiang University, Hangzhou, China, in 1985.

He is currently with State Grid Zhejiang Electric Power Research Institute, Hangzhou, China. His research interests include smart grid, power quality, power system protection, and application of power electronics in power systems.